



## Preparation and Characterization of CaMoO<sub>4</sub> by Solid-State Microwave Metathetic Route

CHANG SUNG LIM

Department of Advanced Materials Science and Engineering, Hanseo University, Seosan 356-706, South Korea

\*Corresponding author: Tel/Fax: +82 41 660 1445; E-mail: cslim@hanseo.ac.kr

(Received: 14 February 2011;

Accepted: 23 November 2011)

AJC-10705

A solid-state metathetic (SSM) route assisted by microwave irradiation was used to synthesize the CaMoO<sub>4</sub> particles in 10 min under environmentally friendly conditions. Well crystallized CaMoO<sub>4</sub> particles were formed at 600 °C for 3 h, showing a fine and homogeneous morphology with sizes of 1-3 μm. The synthesized CaMoO<sub>4</sub> particles were characterized by X-ray diffraction, Fourier transform infrared spectroscopy and scanning electron microscopy. The optical properties were examined by photoluminescence emission and Raman spectroscopy.

**Key Words:** CaMoO<sub>4</sub>, Microwave metathetic synthesis, Luminescence, Raman spectroscopy.

### INTRODUCTION

Metal molybdates have attracted considerable attention for potential applications in photoluminescence, hosts for lanthanide-activated lasers, photocatalysis and humidity sensors<sup>1-3</sup>. The physical, chemical and photochemical properties of metal tungstates are dependent on the manufacturing method. Several processes have been developed over the past decade to enhance the applications of MMoO<sub>4</sub> (M=Ba, Ca, Sr, Pb, Ni, Zn) are prepared by a range of processes, such as co-precipitation<sup>4,5</sup>, electrochemical techniques<sup>6-8</sup>, polymerized complex methods<sup>9</sup>, aqueous mineralization processes<sup>10</sup>, hydrothermal methods<sup>11,12</sup>, microwave-hydrothermal preparations<sup>13-15</sup>, microwave-assisted polymerized complex methods<sup>16-19</sup>, pulsed laser ablation<sup>20</sup>, microwave irradiation<sup>21-23</sup> and solid-state metathetic synthesis<sup>25,26</sup>. Among these methods, wet chemical methods have disadvantages, such as complicated synthetic steps, use of expensive equipment, high synthetic temperatures and long sintering times. On the other hand, solid-state reactions require complex apparatus and techniques, which are becoming gradually unpopular due to the excessive energy consumption.

Compared with the usual methods, microwave synthesis has the advantages of a very short reaction time, small particle size, narrow particle size distribution and high purity method for preparing polycrystalline samples. Microwave heating is delivered to the surface of the material by radiant and/or convection heating, which is transferred to the bulk of the material *via* conduction. Microwave energy is delivered directly to the material through molecular interactions with

an electromagnetic field. Heat can be generated through volumetric heating because microwaves can penetrate the material and supply energy<sup>23,24</sup>. Therefore it is possible to achieve rapid and uniform heating of thick materials. Solid-state synthesis of materials by the metathetic route is a simple and cost-effective method that provides high yield with easy scale up and is emerging as a viable alternative approach for the synthesis of high-quality novel inorganic materials in short time periods.

Metal molybdates exhibit blue or green luminescent spectra, which are based on a radiative transition within the tetrahedral [MoO<sub>4</sub>]<sup>2-</sup> group. However, few studies have reported the microwave metathetic synthesis and luminescent properties of CaMoO<sub>4</sub> particles. Therefore, the precise nature of the optical properties and microwave metathetic synthesis of CaMoO<sub>4</sub> particles is required for a wide range of applications. In this study, CaMoO<sub>4</sub> particles were synthesized using a solid-state metathetic (SSM) method with microwave irradiation. The characteristics of the solid-state metathetic reaction of CaMoO<sub>4</sub> particles are discussed in detail based on the formation of a high lattice energy by-product of NaCl. The synthesized CaMoO<sub>4</sub> particles were characterized by X-ray diffraction (XRD), Fourier transform infrared spectroscopy (FTIR) and scanning electron microscopy (SEM). The optical properties were examined by photoluminescence (PL) emission and Raman spectroscopy.

### EXPERIMENTAL

CaCl<sub>2</sub> and Na<sub>2</sub>MoO<sub>4</sub>·2H<sub>2</sub>O of analytic reagent grade were used to prepare the CaMoO<sub>4</sub>. Fig. 1 shows a flow chart for the

synthesis of  $\text{CaMoO}_4$  particles from the solid-state metathetic method using microwave irradiation. The preparation of calcium molybdate was carried out by reacting well-ground mixtures of  $\text{CaCl}_2$  and  $\text{Na}_2\text{MoO}_4 \cdot 2\text{H}_2\text{O}$  at a molar ratio of 1:1. The sample mixtures were dried at  $100^\circ\text{C}$  for 12 h, placed into crucibles and exposed to domestic microwaves (Samsung Electronics Corp. Korea) operating at a frequency of 2.45 GHz and a maximum out-put power of 1250 W for 10 min. The samples were treated with ultrasonic radiation and washed many times with distilled water and ethanol to remove the  $\text{NaCl}$  reaction by-product. The samples were dried at  $100^\circ\text{C}$  in an oven and heat-treated at  $600^\circ\text{C}$  for 3 h.

The existing phase in the particles after the metathetic reactions and heat-treatment was identified by powder XRD ( $\text{CuK}\alpha$ , 40 kV, 30 mA, Rigaku, Japan) at a scan rate of  $3^\circ/\text{min}$ . FTIR (Model IR 550, Magna, Nicolet Company) was used to examine the thermal-decomposition behaviour of the metathetic reaction and heat-treated particles over the frequency range,  $4000$  to  $400\text{ cm}^{-1}$ . The microstructure and surface morphology of the  $\text{CaMoO}_4$  particles were observed by SEM (JSM-35CF, JEOL). The photoluminescence spectra were recorded using a Hitachi 850 Spectrophotometer (Japan) at room temperature. Raman spectroscopy measurements were performed using LabRam HR (Jobin-Yvon, France). The  $514.5\text{ nm}$  line of an Ar-ion laser was used as excitation source, the power was kept at  $0.5\text{ mW}$  on sample.

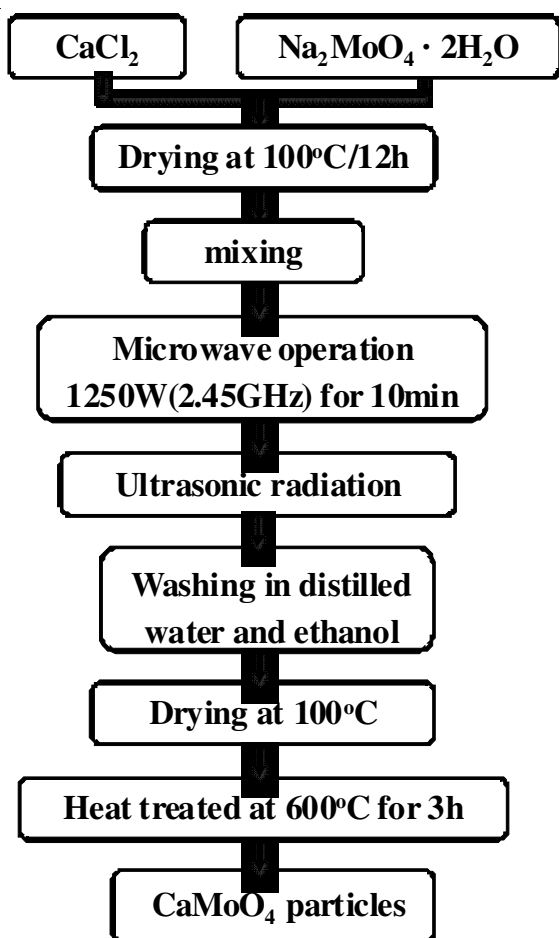


Fig. 1. Flow chart for the synthesis of  $\text{CaMoO}_4$  particles using the SSM method with microwave irradiation

## RESULTS AND DISCUSSION

Fig. 2 shows XRD patterns of the microwave metathetic synthesized  $\text{CaMoO}_4$  particles heat-treated at  $600^\circ\text{C}$  for 3 h. All XRD peaks could be assigned to a tetragonal phase  $\text{CaMoO}_4$  with scheelite-type structure, which is in good agreement with the crystallographic data of  $\text{CaMoO}_4$  (JCPDS: 85-0585). This means that the tetragonal phase  $\text{CaMoO}_4$  can be prepared using this solid-state metathetic reaction assisted by microwave irradiation. The formation of  $\text{CaMoO}_4$  crystalline phases requires heat treatment at  $600^\circ\text{C}$  for 3 h. The  $\text{CaMoO}_4$  formed had a scheelite-type crystal structure<sup>22</sup> with lattice parameters of  $a = b = 5.212\text{ \AA}$  and  $c = 11.438$ . This suggests that solid-state metathetic synthesis is suitable for the growth of  $\text{CaMoO}_4$  crystallites and development of the strongest intensity peaks at (101), (112) and (204) planes.

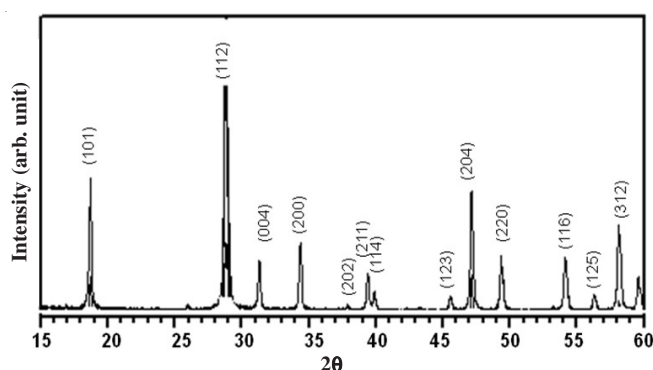


Fig. 2. XRD patterns of the  $\text{CaMoO}_4$  particles

Fig. 3 shows a SEM image of the  $\text{CaMoO}_4$  particles heat-treated at  $600^\circ\text{C}$  for 3 h. The SEM image shows a fine and homogeneous morphology with sizes of  $1\text{--}3\text{ }\mu\text{m}$ . The microwave metathetic synthesis resulted in fine particles with a controlled morphology and the formation of the product in a green manner without the generation of solvent waste, because the microwave radiation provided the energy required to overcome the energy barrier that precludes a spontaneous reaction and helped heat the bulk of the material uniformly. The solid state metathesis reaction, such as  $\text{CaCl}_2 + \text{Na}_2\text{MoO}_4 \rightarrow \text{CaMoO}_4 + 2\text{NaCl}$ , involves the exchange of atomic/ionic species, where the driving force is the formation of a thermodynamically stable alkali or alkaline earth halide with high lattice energy<sup>23,24</sup>. The enthalpy change favours the metathesis reaction and is the driving force for the metathesis involving the formation of  $\text{NaCl}$ <sup>25, 26</sup>. Solid-state metathetic reactions occur so rapidly that all the enthalpy released is essentially used to heat up the solid products. The solid-state metathesis reactions provide convenient route for the synthesis of metal molybdates, which were obtained in the form of loosely connected submicron sized particles at considerably lower temperatures than those usually employed for their synthesis. For molybdate materials to be used for practical applications, control of the particle size distribution and morphology of the particles is needed. The well-defined particle features of the  $\text{CaMoO}_4$  particles synthesized by solid-state metathetic reactions have control over the morphology of the final particles and can be used for such technological applications.

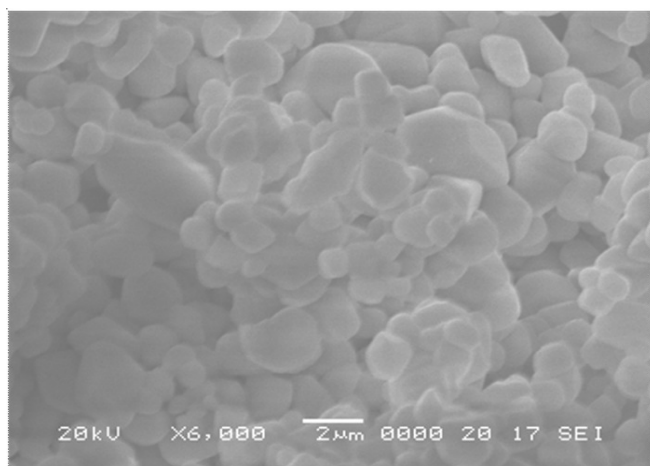


Fig. 3. A SEM image of the CaMoO<sub>4</sub> particles showing the fine and homogeneous morphology with sizes of 1-3 μm

Fig. 4 shows FTIR spectra of the CaMoO<sub>4</sub> particles at the wavenumber range, 4000-480 cm<sup>-1</sup>. The stretching vibration was detected as a strong Mo-O stretch in the [MoO<sub>4</sub>]<sup>2-</sup> tetrahedrons at 974-737 cm<sup>-1</sup>. The [MoO<sub>4</sub>]<sup>2-</sup> is constituted by four internal modes ( $\nu_1(A_1)$ ,  $\nu_2(E)$ ,  $\nu_3(F_2)$  and  $\nu_4(F_2)$ ) specified as an antisymmetric stretching vibration<sup>13</sup>. All modes are Raman active, but  $\nu_3(F_2)$  and  $\nu_4(F_2)$  are IR active. This is one of the internal modes specified as an anti-symmetric stretching vibration.

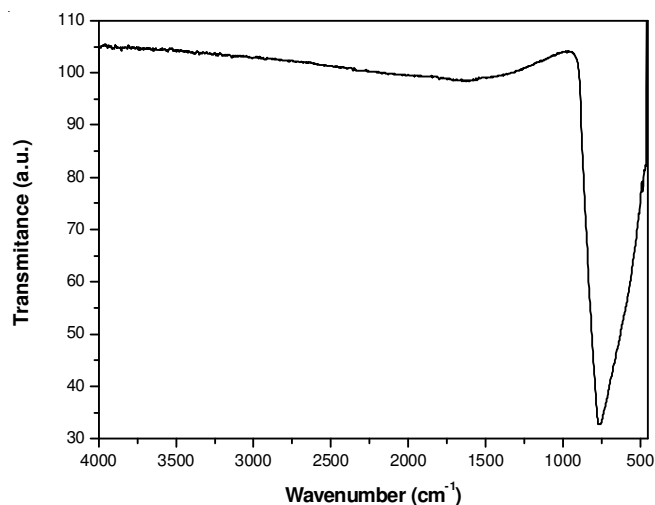


Fig. 4. FT-IR spectra of the CaMoO<sub>4</sub> particles

Fig. 5 presents room-temperature photoluminescence emission spectra of the CaMoO<sub>4</sub> particles. With excitation at 240 nm, the CaMoO<sub>4</sub> particles exhibit a strong photoluminescence emission in the blue wavelength range of 420-430 nm. It is generally assumed that the measured emission spectrum of CaMoO<sub>4</sub> is due mainly to charge-transfer transitions within the [MoO<sub>4</sub>]<sup>2-</sup> complex<sup>27,28</sup>. The photoluminescence intensity of phosphors depends strongly on the particle shape and distribution. Generally, for the similar morphological samples, the homogenized particle must be favourable to luminescent characteristics because of less contamination or fewer dead layers on the phosphor surface. The strong photoluminescence intensity is attributed to the well-defined and homogeneous morphology with sizes of 1-3 μm in Fig. 3.

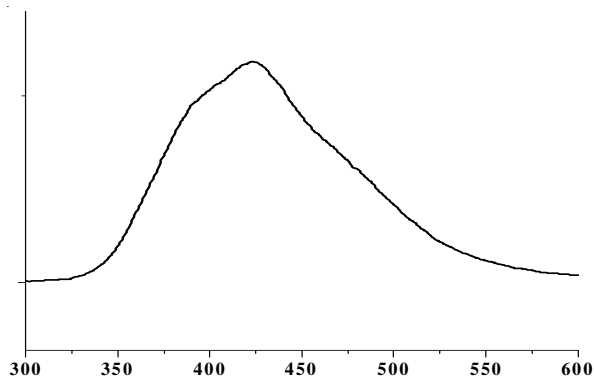


Fig. 5. Photoluminescence emission spectra of the CaMoO<sub>4</sub> particles excited at 240 nm at room temperature

Fig. 6 shows Raman spectra of the CaMoO<sub>4</sub> particle excited 514.5 nm line of an Ar-ion laser kept at 0.5 mW on sample. The vibration modes in the Raman spectra of molybdates are classified into two groups, internal and external<sup>29,30</sup>. The internal vibrations are related to the [MoO<sub>4</sub>]<sup>2-</sup> molecular group with a stationary mass center. The external vibrations or lattice phonons are associated to the motion of the Ca<sup>2+</sup> cation and rigid molecular units. In the free space, [MoO<sub>4</sub>]<sup>2-</sup> tetrahedrons show T<sub>d</sub>-symmetry. In this case, the vibrations of the [MoO<sub>4</sub>]<sup>2-</sup> ions are constituted by four internal modes ( $\nu_1(A_1)$ ,  $\nu_2(E)$ ,  $\nu_3(F_2)$  and  $\nu_4(F_2)$ ), one free rotation mode ( $\nu_5(F_1)$ ) and one transition mode ( $F_2$ ). When [MoO<sub>4</sub>]<sup>2-</sup> ions are present in a scheelite-type structure, its point symmetry reduces to S<sub>4</sub>. Therefore, all degenerative vibrations are split due to the crystal field effect. For a tetragonal scheelite primitive cell with a  $\mathbf{k} = \mathbf{0}$  wavevector<sup>13,28</sup>, there are 26 different vibrations ( $\Gamma = 3A_g + 5A_u + 5B_g + 3B_u + 5E_g + 5E_u$ ), as determined by group-theory calculations. Among them, the 3A<sub>g</sub>, 5B<sub>g</sub> and 5E<sub>g</sub> vibrations are Raman-active. Only 4A<sub>u</sub> and 4E<sub>u</sub> of the 5A<sub>u</sub> and 5E<sub>u</sub> vibrations are active in the IR frequencies and the remaining (1A<sub>u</sub> and 1E<sub>u</sub>) are acoustic vibrations. The 3B<sub>u</sub> vibration is a silent mode. The Raman modes for the CaMoO<sub>4</sub> particles in Fig. 6 were detected as  $\nu_1(A_g)$ ,  $\nu_3(B_g)$ ,  $\nu_3(E_g)$ ,  $\nu_4(E_g)$ ,  $\nu_4(B_g)$  and  $\nu_2(B_g)$  vibrations at 925, 831, 795, 352, 344 and 332 cm<sup>-1</sup>, respectively, which provide evidence of a scheelite structure. The well-resolved sharp peaks for the CaMoO<sub>4</sub> particles indicate that the synthesized particles are highly crystallized. The free rotation mode was detected at 189 cm<sup>-1</sup> and the external mode was localized at 148 cm<sup>-1</sup>. The internal vibration mode frequencies exhibited dependence on lattice parameters and the degree of the partially covalent bond between the cation and molecular ionic group [MoO<sub>4</sub>]<sup>2-</sup>. The sort of cations (Ca<sup>2+</sup>, Sr<sup>2+</sup>, Ba<sup>2+</sup>) can influence on the Raman modes by changing the size of the crystal unit cell and by covalent cation effect<sup>30</sup>. The essential dependence of the bandwidth of  $\nu_1(A_g)$  Raman mode on the peculiarities of crystal lattice and the type of Me<sup>2+</sup> cation in the series of MMoO<sub>4</sub> (M= Ca, Sr, Ba, Pb) crystals with scheelite structure. The moving in the series of molybdates Ca<sup>2+</sup> → Sr<sup>2+</sup> → Ba<sup>2+</sup> increases the unit cell and interionic distance inside the molecular group. The degree of covalent bond between the cation and molecular group usually decreases within the series Ca<sup>2+</sup> → Sr<sup>2+</sup> → Ba<sup>2+</sup>. This anomalous phenomenon can be explained by decreasing of interaction between internal and external Raman modes in scheelite structure in molybdates.

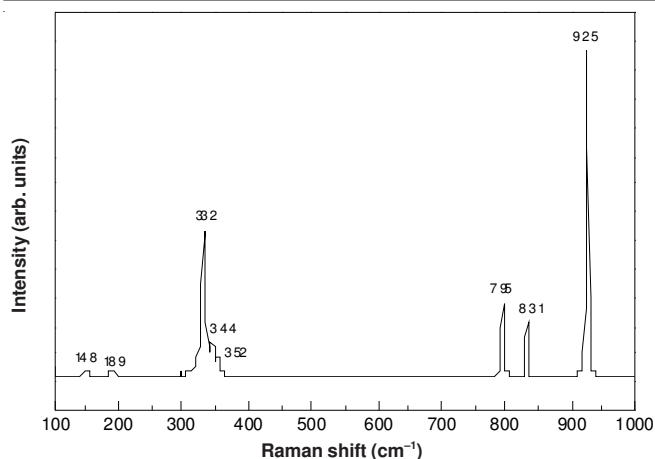


Fig. 6. Raman spectra of the  $\text{CaMoO}_4$  particles excited by the 514.5 nm line of an Ar-ion laser at 0.5 mW on sample

## Conclusion

The  $\text{CaMoO}_4$  particles were well crystallized by the solid-state metathetic method with microwave irradiation, showing the fine and homogeneous morphology with sizes of 1-3  $\mu\text{m}$ . The stretching vibration in FTIR was detected as a strong Mo-O stretch in the  $[\text{MoO}_4]^{2-}$  tetrahedrons at 737-974  $\text{cm}^{-1}$ . With excitation at 240 nm, the  $\text{CaMoO}_4$  particles exhibit a strong photoluminescence emission in the blue wavelength range of 420-430 nm. The strong photoluminescence intensity is attributed to the well-defined and homogeneous particle morphology. The well-resolved Raman spectra at 925, 831, 795, 352, 344 and 332  $\text{cm}^{-1}$  for the  $\text{CaMoO}_4$  particles indicate that the synthesized particles are highly crystallized. The free rotation mode was detected at 189  $\text{cm}^{-1}$  and the external mode was localized at 148  $\text{cm}^{-1}$ .

## ACKNOWLEDGEMENTS

This study was supported by Basic Science Research Program through the National Research Foundation of Korea (NRF) funded by the Ministry of Education, Science and Technology (2011-0026911).

## REFERENCES

1. R. Sundaram and K.S. Nagaraja, *Sens. Actuators B*, **101**, 353 (2004).
2. L. Zhen, W.S. Wang, C.Y. Xu, W.Z. Shao, M.M. Ye and Z.L. Chen, *Scripta Mater.*, **58**, 461 (2008).

3. R.N. Singh, J.P. Singh and A. Singh, *Int. J. Hydrogen Ener.*, **33**, 4260 (2008).
4. X. Zhao, T.L.Y. Cheung, Y. Xi, K.C. Chung, D.H.L. Ng and J. Yu, *J. Mater. Sci.*, **42**, 6716 (2007).
5. T. Thongtem, S. Kungwankunakorn, B. Kuntalue, A. Phuruangrat and S. Thongtem, *J. Alloys Compd.*, **506**, 475 (2010).
6. P. Yu, J. Bi, D.J. Gao, Q. Xiao, L.P. Chen, X.L. Jin and Z.N. Yang, *J. Electroceram.*, **21**, 184 (2008).
7. P. Yu, J. Bi, D.Q. Xiao, L.P. Chen, X.L. Jin and Z.N. Yang, *J. Electroceram.*, **16**, 473 (2006).
8. Y. Sun, J. Ma, J. Fang, C. Gao and Z. Liu, *Ceram. Inter.*, **37**, 683 (2011).
9. J.W. Yoon, J.H. Ryu and K.B. Shim, *Mater. Sci. Eng. B*, **127**, 154 (2006).
10. X. Wu, J. Du, H. Li, M. Zhang, B. Xi, H. Fan, Y. Zhu and Y. Qian, *J. Sol. State Chem.*, **180**, 3288 (2007).
11. G. Zhang, S. Yu, Y. Yang, W. Jiang, S. Zhang and B. Huang, *J. Cryst. Growth*, **312**, 1866 (2010).
12. K. Eda, Y. Kato, Y. Ohshiro, T. Sugitani and M.S. Whittingham, *J. Solid State Chem.*, **183**, 1334 (2010).
13. J.T. Kloprogge, M.L. Weier, L.V. Duong and R.L. Frost, *Mater. Chem. Phys.*, **88**, 438 (2004).
14. J.C. Sczancoski, L.S. Cavalcante, M.R. Joya, J.A. Varela, P.S. Pizani and E. Longo, *Chem. Eng. J.*, **140**, 632 (2008).
15. L.S. Cavalcante, J.C. Sczancoski, R.L. Tranquilin, J.A. Varela, E. Longo and M.O. Orlandi, *Particuology*, **7**, 353 (2009).
16. J.H. Ryu, J.W. Yoon, C.S. Lim, W.C. Oh and K.B. Shim, *J. Alloys Compd.*, **390**, 245 (2005).
17. J.H. Ryu, B.G. Choi, S.H. Kim, J.W. Yoon, C.S. Lim and K.B. Shim, *Mater. Res. Bull.*, **40**, 1468 (2005).
18. J.H. Ryu, S.M. Koo, J.W. Yoon, C.S. Lim and K.B. Shim, *Mater. Lett.*, **60**, 1702 (2006).
19. J.H. Ryu, B.G. Choi, S.H. Kim, J.W. Yoon, C.S. Lim and K.B. Shim, *J. Mater. Sci.*, **40**, 4979 (2005).
20. J.H. Ryu, B.G. Choi, J.W. Yoon, K.B. Shim, K. Machi and K. Hamada, *J. Lum.*, **67**, 124 (2007).
21. T. Thongtem and A. Phuruangrat, *J. Nanopart. Res.*, **12**, 2287 (2010).
22. T. Thongtem, A. Phuruangrat and S. Thongtem, *Mater. Lett.*, **62**, 454 (2008).
23. S. Das, A.K. Mukhopadhyay, S. Datta and D. Basu, *Bull. Mater. Sci.*, **32**, 1 (2009).
24. K.P.F. Siqueira, R.L. Moreira, M. Valadares and A. Dias, *J. Mater. Sci.*, **45**, 6083 (2010).
25. P. Parhi, S.S. Singh, A.R. Ray and A. Ramanan, *Bull. Mater. Sci.*, **29**, 115 (2006).
26. V. Thangadurai, C. Knittlmayer and W. Weppner, *Mater. Sci. Eng. B*, **106**, 228 (2004).
27. D.A. Spassky, S.N. Ivanov, V.N. Kolobanov, V.V. Mikhailin, V.N. Zemskov, B.I. Zadneprovski and L.I. Potkin, *Radiat. Meas.*, **38**, 607 (2004).
28. G.Y. Hong, B.S. Jeon, Y.K. Yoo and J.S. Yoo, *J. Electro. Soc.*, **148**, H161 (2001).
29. T.T. Basiev, A.A. Sobol, Y.K. Voronko and P.G. Zverev, *Opt. Mater.*, **15**, 205 (2000).
30. T.T. Basiev, A.A. Sobol, P.G. Zverev, L.I. Ivleva, V.V. Osiko and R.C. Powell, *Opt. Mater.*, **11**, 307 (1999).